Journal of Geographic Information System, 2025, 17(1), 97-117
https://www.scirp.org/journal/jgis
ISSN Online: 2151-1969
ISSN Print: 2151-1950

Modelling Land Degradation (LD) Using Geospatial Techniques for Agricultural and Environmental Management Case Study: Alla Catchment; Dekemhare-Eritrea

Okbaldet Negede*, Faith Njoki Karanja

Department of Geospatial and Space Technology, University of Nairobi, Nairobi, Kenya
Email: *okbaldetn@gmail.com

How to cite this paper: Negede, O. and Karanja, F.N. (2025) Modelling Land Degradation (LD) Using Geospatial Techniques for Agricultural and Environmental Management Case Study: Alla Catchment; Dekemhare-Eritrea. *Journal of Geographic Information System*, **17**, 97-117.
https://doi.org/10.4236/jgis.2025.171006

Received: January 19, 2025
Accepted: February 25, 2025
Published: February 28, 2025

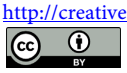

Abstract

Eritrea faces significant environmental and agricultural challenges due to human activities, rugged terrain, and fluctuating climates like recurrent droughts and erratic rainfall. Desertification, deforestation, and soil erosion are major concerns affecting soil quality, water resources, and vegetation, especially in areas like the Alla catchment. Recent assessments reveal declining vegetation and precipitation levels over four decades, alongside rising temperatures, linked to increased desertification and land degradation driven by climate variations and prolonged droughts. The urgent need for sustainable land management practices is explained by reduced productivity, biodiversity, and ecosystem health. This study focused on modelling land degradation in Eritrea's Alla catchment using advanced geospatial techniques. Vegetation indices and soil erosion models were used to evaluate critical factors such as rainfall Erosivity, soil erodibility, slope characteristics, and land cover management. The resulting model highlighted varying levels of susceptibility to land degradation, highlighting widespread vulnerability characterized by high and very high susceptibility hotspots. Areas with minimal degradation were found in the northern vegetation-covered regions. Soil loss in the catchment is primarily influenced by inadequate land cover, steep slopes, soil erosion susceptibility, erosive rainfall patterns, and insufficient support practices. The study underscores the urgency of addressing deforestation and unsustainable agricultural practices to mitigate soil erosion. Recommendations include enhancing community capacity for effective land management, promoting climate adaptation strategies, and aligning national efforts with the global Sustainable Development Goals to achieve Land Degradation Neutrality.

Keywords

Alla Catchment, Remote Sensing, Google Earth Pro, NDVI, LULC, Land Degradation, Sustainable Development Goals, Soil Erosion, Susceptibility Map

1. Introduction

1.1. Background

Globally, about 25% of arable land is currently degraded, with an additional 12 million hectares being degraded annually, resulting in substantial economic losses estimated at USD 490 billion per year. This degradation impacts global agricultural GDP by 3% to 6% [1]-[3]. In Eritrea, the problem has escalated due to historical mismanagement of agricultural resources and exacerbated by factors such as population growth, unsustainable farming practices, has been an increase in livestock numbers, soil erosion, and climate variations. These issues collectively diminish the land's capacity to support both current and future generations that agrarian and pastoral activities, such as intensive farming and overgrazing, contribute to land degradation through deforestation, vegetation loss, soil erosion, and compaction, with remote sensing data showing higher degradation in areas with these pressures.

In an effort to address these challenges and alleviate poverty, the Government of Eritrea, in partnership with the International Fund for Agricultural Development (IFAD) and the Global Environment Facility (GEF), launched the "Catchment and Land Management Project" (CLMP). This initiative aims to succeed the Post-Crisis Rural Recovery and Development Programme (PCRRDP) in the Gash-Barka and Southern Region, supported by a GEF grant since its inception mission in 2008 (IFAD-GEF Project ID 3362). The project focuses on sustainable land management practices to mitigate degradation caused by deforestation, desertification, and unsustainable land-use practices driven by energy demands.

In Africa, soil erosion leads to an annual decline in productivity ranging from 2% to 40%, averaging 8.2% across the continent, highlighting the severity of land degradation issues [3] [4]. Eritrea faces similar challenges where factors like conflict, deforestation, and desertification exacerbate land degradation, impacting many livelihoods. Climate variability further strains ecosystem resilience and the sustainability of livelihoods [5] [6]. Comprehensive assessments and strategic interventions are urgently needed at the catchment level, providing essential data for policymakers to develop effective strategies ensuring food and water security, environmental preservation, and sustainable economic growth [7].

Land degradation results from various factors, including severe weather conditions-particularly drought-as well as human activities that contribute to soil deterioration. Additionally, certain land use practices adversely impact food production and livelihoods. Desertification, a specific form of land degradation, transforms

once-fertile land into arid desert. According to the World Resources Institute (1992-1993), over the past 45 years, an area equivalent in size to China and India has experienced moderate to severe soil degradation [8] [9].

1.2. Land Degradation

Land degradation is a process driven by human activities and climate change which includes soil erosion, desertification, deforestation, and biodiversity loss, reducing land productivity and ecosystem services [10]. Unsustainable practices like overgrazing and deforestation for agriculture exacerbate the situation, resulting in reduced agricultural productivity and increased vulnerability to natural disasters. In Eritrea, soil erosion, particularly in the Central Highlands and the study area, is more pronounced due to intense rainfall, rugged terrain, overgrazing, and deforestation [11] [12]. The Mogogo Adhanet stove helps mitigate deforestation and smoke pollution by conserving 80% of firewood. Addressing land degradation requires sustainable management, conservation strategies, and international cooperation [13] [14].

1.3. Role of Geospatial Techniques for Modelling Land Degradation

Geospatial techniques provide a structured approach to model and monitor land degradation, aiding in proactive management and conservation. In general, the process of modelling land degradation involves identifying indicators for land degradation (soil erosion, vegetation loss); collecting relevant geospatial data (satellite imagery, climate data, etc.) and the extraction of indicator factor maps. The indicator factor maps are then integrated into a spatial framework to generate land degradation risk map and models that reflect susceptibility patterns. Stakeholders' engagement during the land degradation mapping ensures expert views are incorporated while validating the land susceptibility maps generated.

To address and ideally reverse the land degradation, it is important to enhance national capabilities for assessing and mapping degraded lands, as recommended by the United Nations Sustainable Development Goals (SDGs). Indicator 15.3.1, which tracks the "proportion of land that is degraded over total land area," requires countries to regularly produce data to monitor and evaluate changes over time. Earth Observations (EO) can significantly contribute by providing necessary data in countries where it is absent and by supplementing and improving national data sources [15].

[16] undertook a study to enhance knowledge through earth observations in support of the Sustainable Development Goals, particularly target 15.3.1. They employed "trends.earth", a free geospatial technology tool available on the QGIS platform, to monitor surface trends.

RUSLE has garnered widespread application across diverse regions and scales, ranging from individual fields to expansive watersheds and agricultural landscapes. It has been used in North Western Ethiopia to assess soil erosion [17] and Morocco to estimate soil erosion risks [18]. Its primary purpose is to evaluate soil

erosion risk and inform land management strategies. Typically, RUSLE is integrated with complementary models such as GIS platforms, and hydrological models, alongside online validations and local expertise, to enhance its predictive accuracy and reliability in assessing land degradation [19]. It has been employed for soil erosion assessment and modelling, as explained in Equations (1) to (8).

$$A = R * K * LS * C * P \tag{1}$$

where A = Average annual soil loss (t/ha/yr), R = Rainfall Erosivity factor, K = Soil erodibility factor, LS = Slope length and steepness factor, C = Cover management factor, and P = Support practice factor

1) Rainfall Erosivity Factor (R): Rainfall and runoff play an important role in the soil erosion process and are usually expressed as the R factor. The greater the rain storm's intensity and duration (depth), the higher the erosion potential [20]. It is a factor that quantifies the erosive force of the rainfall in an area, in which high-intensity rainfall causes more soil erosion [21]. To determine the Rainfall Erosivity factor (R), one common formula practiced in the Horn of Africa (especially Eritrea and Ethiopia) [22] is as shown in Equation (2).

$$R = -8.12 + \left(0.526 * P\right) \tag{2}$$

where R is the rainfall Erosivity factor, and P is the annual precipitation.

2) Soil Erodibility Factor (K): The soil erodibility factor (K) represents the susceptibility of the soil to erosion by taking into account the soil texture, and organic matter content. It reflects the ease with which the soil is detached by splash during rainfall and/or by surface runoff and therefore shows the change in the soil per unit of applied external force of energy [22]. It is related to the integrated effects of rainfall, runoff, and infiltration on soil loss, accounting for the influences of soil properties on soil loss during storm events in upland areas [23]. The entire study area is divided into two classes based on the soil texture and hence the K-values: Humic Cambisols (Bh) and Lithosols (I) [24].

The K-Factor values are derived as shown in Equations (3) to (7) [25].

$$K_{usle} = f_{csand} * f_{cl-si} * f_{orgc} * f_{hisand} \tag{3}$$

$$f_{csand} = 0.2 + 0.3 * \mathrm{e}^{-0.256 * m_s \left(1 - m_{silt}/100\right)} \tag{4}$$

$$f_{cl-si} = \left(m_{silt} / \left(m_c + m_{silt}\right)\right)^{0.3} \tag{5}$$

$$f_{org} = 1 - 0.25 * orgc + \mathrm{e}^{3.72 - 2.95 * orgc} \tag{6}$$

$$f_{hisand} = 1 - \frac{0.7 * \frac{1 - m_s}{100}}{\frac{1 - m_s}{100}} + \mathrm{e}^{-5.51 + 22.9 * \frac{1 - m_s}{100}} \tag{7}$$

where, K_{usle} is the erodibility factor, M_s is the % sand, M_{silt} is the % silt, M_c is the % clay, and $Orgc$ is the % organic matter.

3) Slope length and steepness Factor (LS): This represents the combined effect of slope length (L) and slope steepness (S) on soil erosion as shown in Equation (8). This factor is crucial in modelling and predicting soil erosion rates as it quantifies

the influence of topography on erosion processes. The slope length factor (L) measures the distance from the origin of overland flow to the point where either the slope decreases to the extent that deposition begins or runoff becomes concentrated in a defined channel. The slope steepness factor (S) indicates the influence of the slope's angle on erosion. The longer the slope, the more potential for water to accumulate, which can increase erosion, and Steeper slopes generally lead to faster-moving water, which has more energy and thus a greater capacity to erode the soil [26].

$$LS = power\left(flowaccumulation * \frac{cellsize}{22.13}\right)^{n} * power\left(\sin\left(slope * 0.01745\right)/0.09\right)^{m} \quad (8)$$

where LS is the slope length-steepness factor, and m and n are exponents; $m = 0.6$ (a range between 0.4 and 0.6) and $n = 1.3$ (a range between 1.0 and 1.3). [27].

4) Vegetation cover management Factor (C): The vegetation cover management factor (C) is used to express the effect of plants and soil cover. Plants can reduce the runoff velocity and protect surface pores. Since satellite image data provide up-to-date information on land cover, the use of satellite images in the preparation of land cover maps is widely applied in natural resource surveys [28].

In determining the C factor, the LULC maps are generated and the values assigned between 0 (implies very strong cover effects) and 1 (indicates no cover present and the surface is treated as barren land) [17].

5) Support Practice Factor (P): In determining the Support Practice Factor-P, the entire land of the catchment is classified into 2 classes: Agricultural land and Non-agricultural land [29]. Further, the agricultural land is divided into several classes based on their slope percentages. Agricultural land with greater than 100% slope and Non-agricultural land are combined and so-called other lands having P-value 1, but the agricultural land ranging from 0 to 100% slope is considered as agricultural land with their assigned P-values (0.1 up to 0.33) depending on their percentage slope.

In this study, P-values used are shown in Table 1.

Table 1. P-values.

Land-use type	Slope (%)	P factor value
Agricultural land	0 - 5	0.1
	5 - 10	0.12
	10 - 20	0.14
	20 - 30	0.19
	30 - 50	0.25
	50 - 100	0.33
Other land	All	1

Source: [30].

2. Modelling Land Degradation for Alla Catchment, Dekemhare-Eritrea

2.1. Study Area

The study area (Keyih kor-Gadien/Alla and environs) generally called Alla Catchment, with approximately 208 km^2 of aerial coverage, is found in the Sub-Regional administration of Dekemhare, Southern Region of the country, as shown in Figure 1. It is confined within the UTM coordinates of 1,666,000 to 1,684,000 in latitude and 500,000 to 517,000 in longitude. Gadien, the administrative center of Alla, is about 57 km from Asmara and can be accessed through Dekemhare along the main highway of Asmara-Dekemhare-Gadien-Nefasit-Asmara loop.

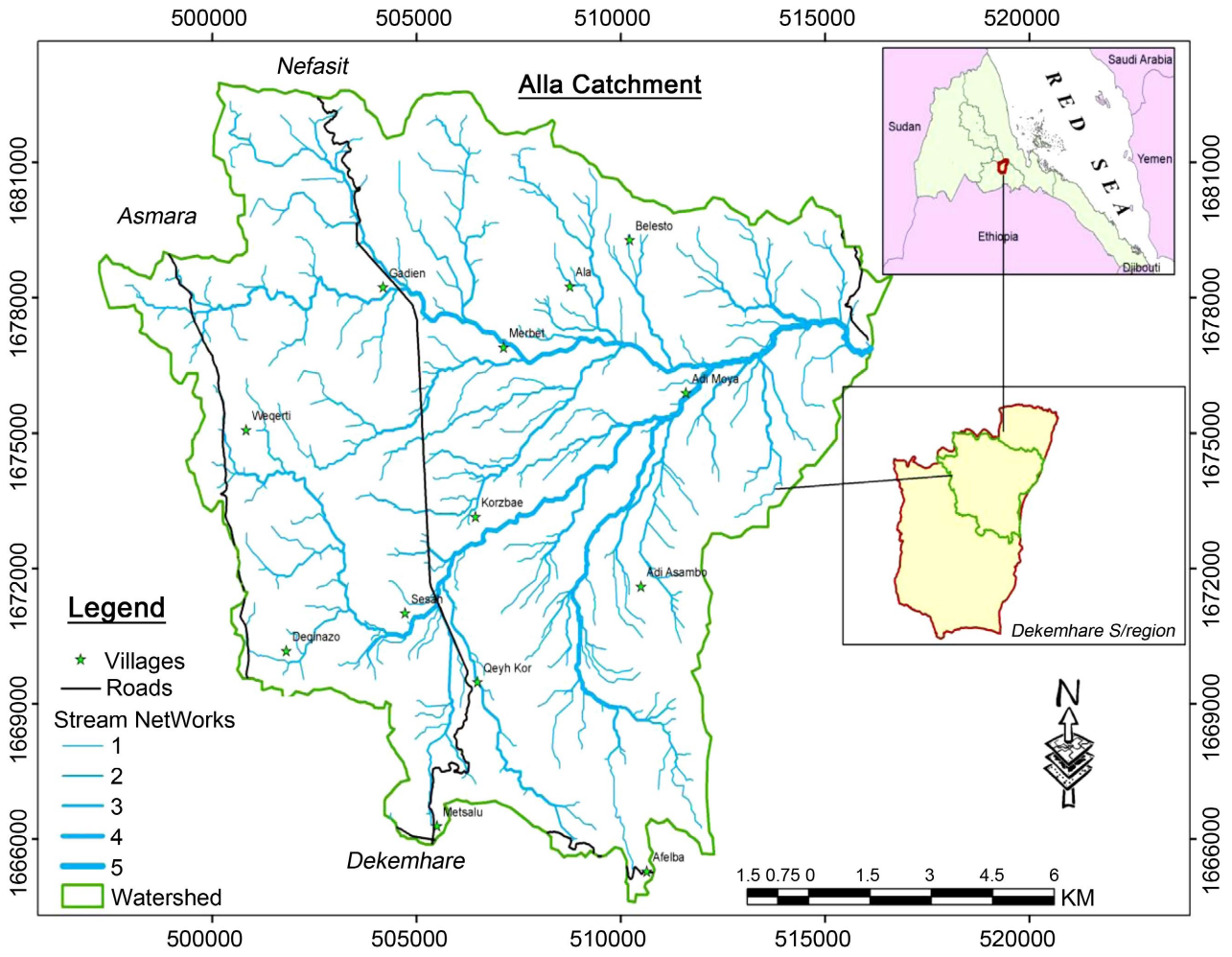

Figure 1. Study area.

The Alla Catchment, is situated on the outskirts of Asmara's (the capital city) eastern plateau. The elevated regions define the outer zone of the area, sloping down to the plain-steeply in some places and more gradually in others. This major morphological feature of Alla is attributed to the result of Red Sea tectonics. Except for isolated hills like Basit Hill, which is 1731 m high, no elevation contrast is

observed on the plain. The continuous process of erosion and weathering has contributed to the effect of the present geomorphologic feature and land deterioration. The climate of the area, unlike the adjacent highlands, is warm as it lies at a lower altitude. However, the annual precipitation is similar to the highland areas which ranges between 500 mm - 800 mm. Annual mean temperature roughly ranges between 20˚C to 30˚C. The mean annual potential evapotranspiration is 1800 mm. The vegetation cover is scarce with acacia and scrub trees being predominant, in addition to the fruit plantations like orange, and papaya, among others. Most of the soil is bare, easily detachable, and characterized as sandy loam with more sand.

The inhabitants of Alla are Tigrigna, Saho, and Tigre, who are mostly agrarians and pastorals. Their economic activities depend on selling agricultural products, sand, and animals for Dekemhare and Asmara. In addition to the cash fruits, crops mainly Taff and sorghum are cultivated in the area.

2.2. Methodology

Identification of key drivers of land degradation guided the selection of appropriate tools and methodologies for modelling. Crucial datasets used included shapefiles data from the Eritrean Mapping and Information Centre, Landsat imagery and elevation data from USGS. Specifically, different data sets used; soil, rainfall, DEM and satellite imagery. Soil erodibility, rainfall erosivity, slope, cover and management were extracted from the soil, rainfall and DEM data respectively. Vegetation cover and land use changes were mapped from Landsat image data. In determining the R factor, the annual precipitation data was downloaded from the Climate Research Unit (CRU) datasets. These variables were then used to generate a land degradation model for each year considered in the study namely 1991, 2000, 2010 and 2020 from which a land susceptibility map of the area was created. Figure 2 is a representation of the methodology overview.

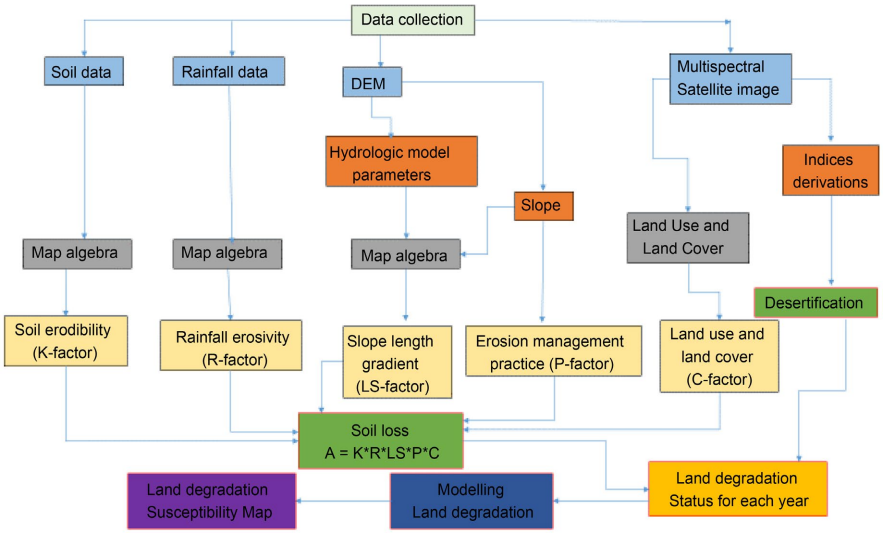

Figure 2. Methodology overview.

These datasets facilitated the derivation of critical factors of the RUSLE model. Vegetation indices such as NDVI, VCI, and SAVI were also computed to assess vegetation health and detect areas affected by desertification.

Using ArcGIS's Model Builder, the annual soil loss rates (t/ha/yr.) from the RUSLE and NDVI values were computed. This data-driven approach enabled the mapping of annual land degradation status and the development of a susceptibility model, highlighting high-risk areas useful in guiding targeted conservation efforts.

3. Results

3.1. Factor Maps

Soil Loss from RUSLE: GIS and erosion models were employed to assess the severity and spatial distribution of land degradation, focusing on erosion from surface runoff and desertification in the Alla Catchment. Five key erosion risk factors; Rainfall erosivity (R), Soil erodibility (K), Slope length and steepness (LS), Cover management (C), and Management practices (P) are presented. Figure 3 presents the Rainfall Erosivity Factor (R) Maps for the years 1991, 2000, 2010 and 2020.

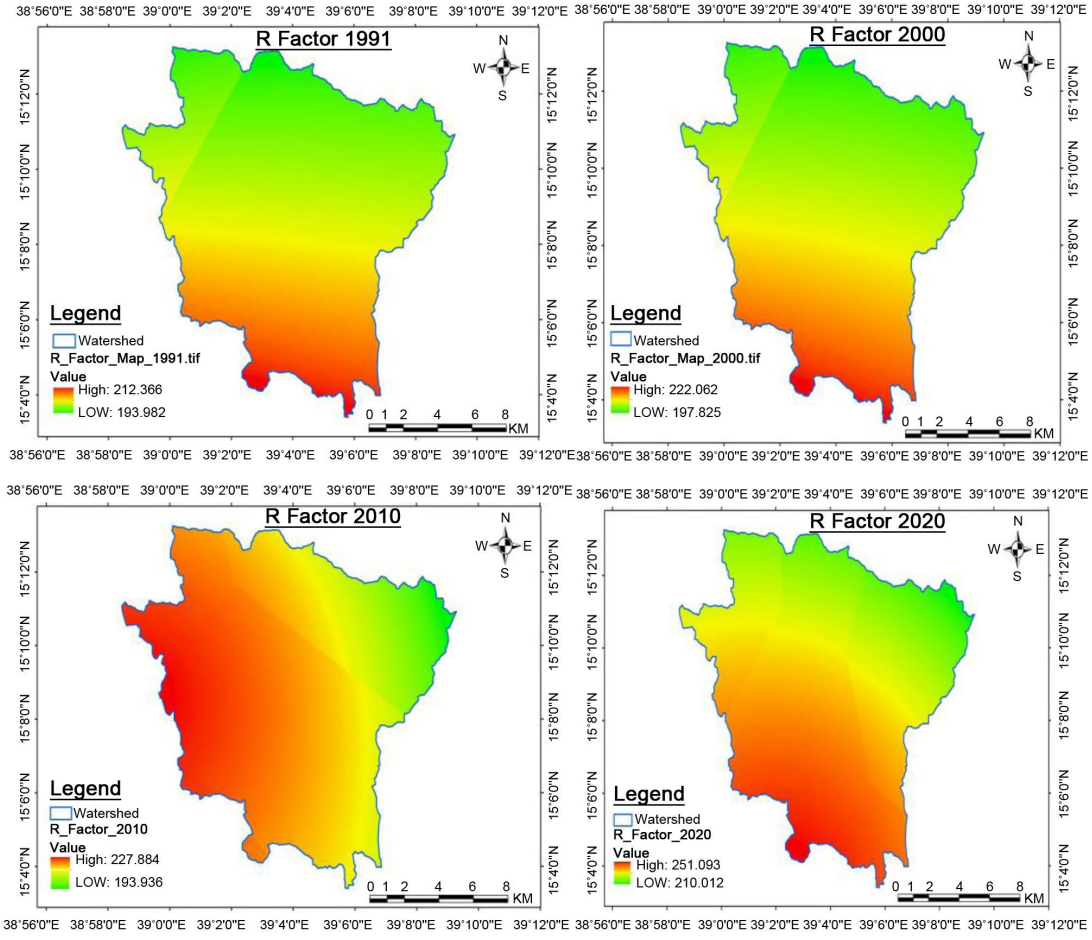

Figure 3. Rainfall erosivity factor (R) Maps (1991, 2000, 2010, 2020).

For the year 2020, which experienced the highest rainfall, the dataset recorded a maximum precipitation of 461.234 mm and a minimum of 388.136 mm. In contrast, for the year 1991, which received the lowest average precipitation, the dataset indicated maximum values of 392.323 mm and minimum values of 359.612 mm. The R factor values that were computed show that the highest values observed were for the year 2020 ranging from 210.012 to 251.093, and the lowest values obtained in 1991 ranging from 193.982 to 212.366. Figure 4 shows the generated Soil Erodibility Factor (K) Maps for the epochs 1991, 2000, 2010 and 2020.

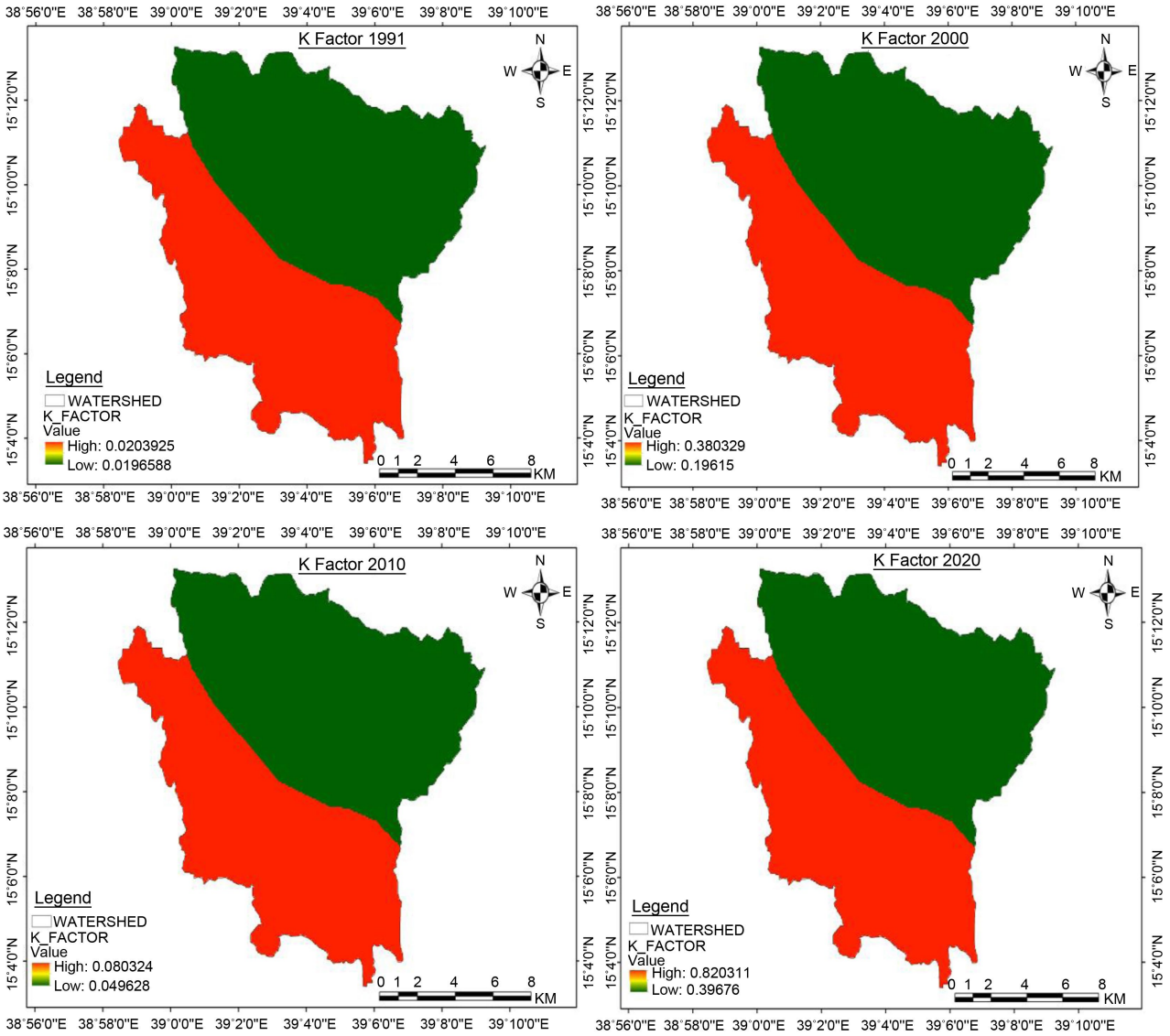

Figure 4. Soil erodibility factor (K) Maps (1991, 2000, 2010, 2020).

The K-factor values reveal that 2020 exhibited the highest values (0.8 for high and 0.3 for low), while 1991 showed the lowest values (0.02 for high and 0.01 for low).

The Slope Length and Steepness Factor (LS) Map is shown in Figure 5.

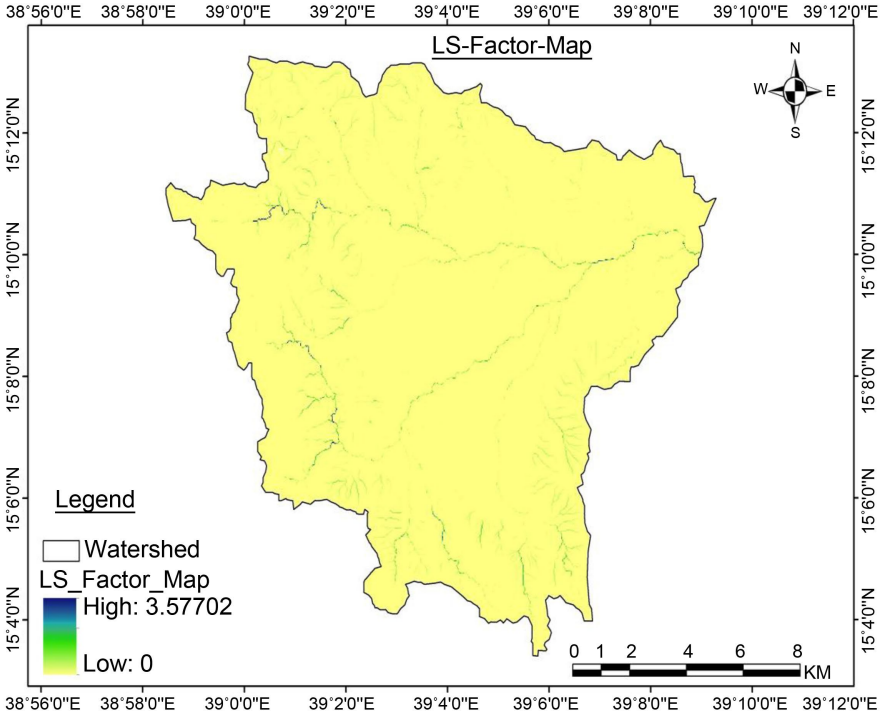

Figure 5. Slope length and steepness factor (LS) map.

The slope of the study area was assessed, and the results are ranging from 0 to 192.205%. Additionally, the flow accumulation of the area was computed, which, when combined with the slope values and Digital Elevation Model (DEM) of 30 m resolution, enabled the determination of the LS factor. The LS factor of the area derived, indicates the highest value recorded as 3.777 and the lowest value as 0.

The Cover and Management Factor (C) and LULC Maps for the years 1991, 2000, 2010 and 20220 are presented in **Figure 6** and **Figure 7** respectively. This factor reflects the effect of LULC, cropping, and management practices on the rate of soil erosion. According to different studies, the values of LULC were assigned where the C-factor values range between 0 (implies very strong cover effects) and 1 (indicates no cover present and the surface is treated as barren land) [17].

This factor indicates the influence of land use and land cover (LULC), cropping patterns, and management practices on soil erosion rates. According to various studies, LULC values were assigned with C-factor values ranging from 0 (indicating strong protective cover) to 1 (representing no cover, treated as barren land).

When comparing the years 1991, 2000, 2010, and 2020, shifts in c-values occurred due to the conversion of certain areas into agricultural and bare lands, ultimately leading to a significant expansion of agricultural land and reducing of vegetation covers.

Comparing multiple Landsat images from different time periods with historical data or regional change assessments were used to evaluate the consistency and reliability of land-use change detection.

When comparing the years 1991, 2000, 2010, and 2020, the LULC maps reveal

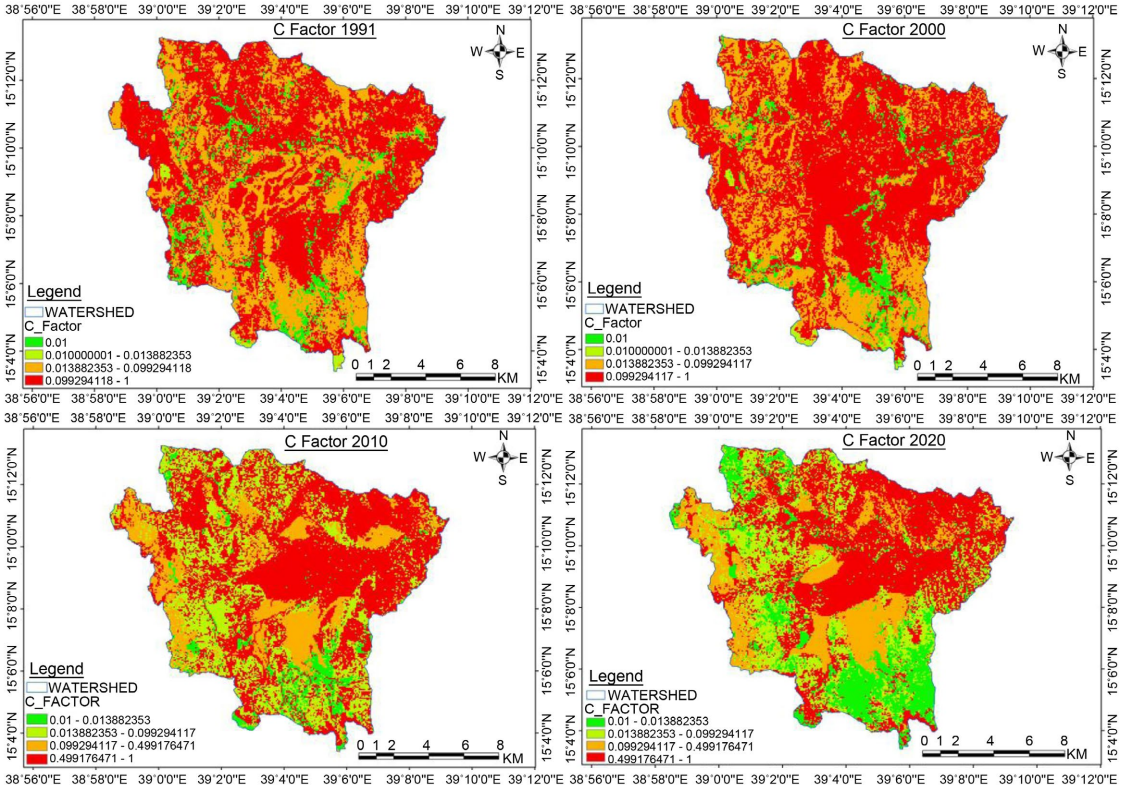

Figure 6. Cover and management factor (C) maps (1991, 2000, 2010, 2020).

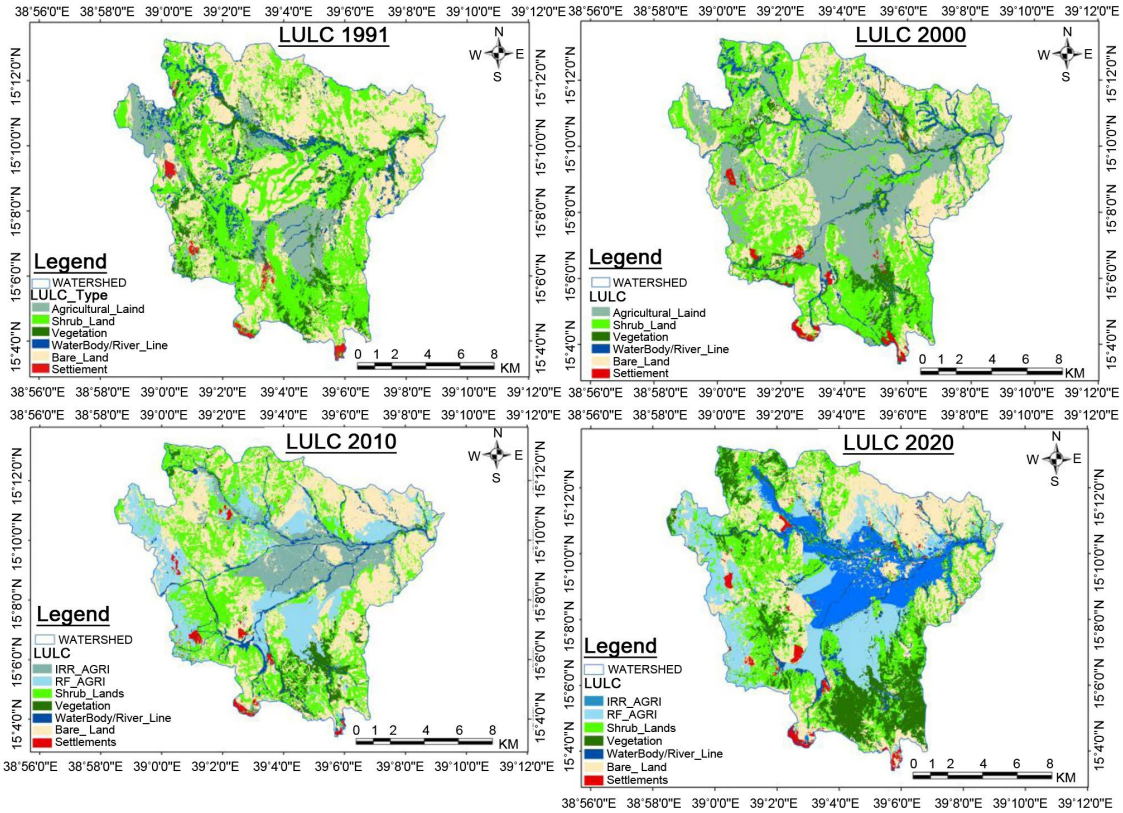

Figure 7. LULC maps (1991, 2000, 2010, 2020).

a gradual shift in land use and cover, indicating that more areas have been converted to agricultural lands (by increasing deforestation) and bare lands (as a result of drought). This has ultimately led to increased desertification. Figure 8 and Figure 9 show the Support Practice Factor (P) and Slope Overlay Maps respectively.

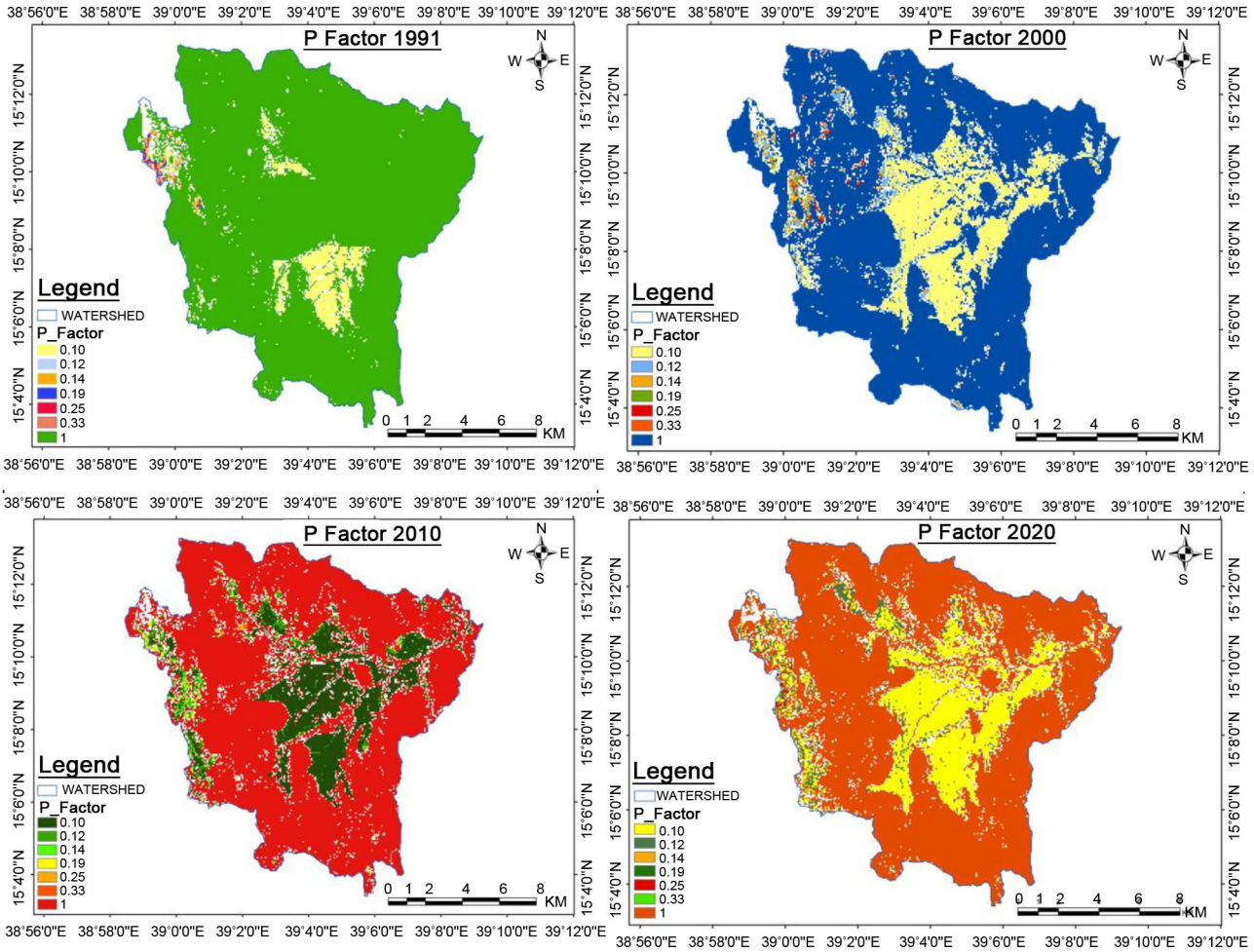

Figure 8. Support practice factor (P) maps (1991, 2000, 2010, 2020).

Drawing from the calculated P-Factor values for each year the four maps generated show a progressive increase in agricultural land from 1991 to 2020. Initially, certain flat and non-agricultural regions were categorized as other land types, but they were reclassified as agricultural land after being converted for farming. As a result, the 2020 map displays a significant expansion of agricultural areas.

Overlay P-Factor Slope refers to the process of overlaying or combining P-factor values with slope data across a landscape. The resulting layer can be used to evaluate the effectiveness of conservation practices on different slopes, helping to identify areas that are more or less susceptible to erosion. Slopes from 0 to 100% are classified as agricultural lands, whereas agricultural lands with slopes exceeding 100% along with land uses other than agriculture are categorized as

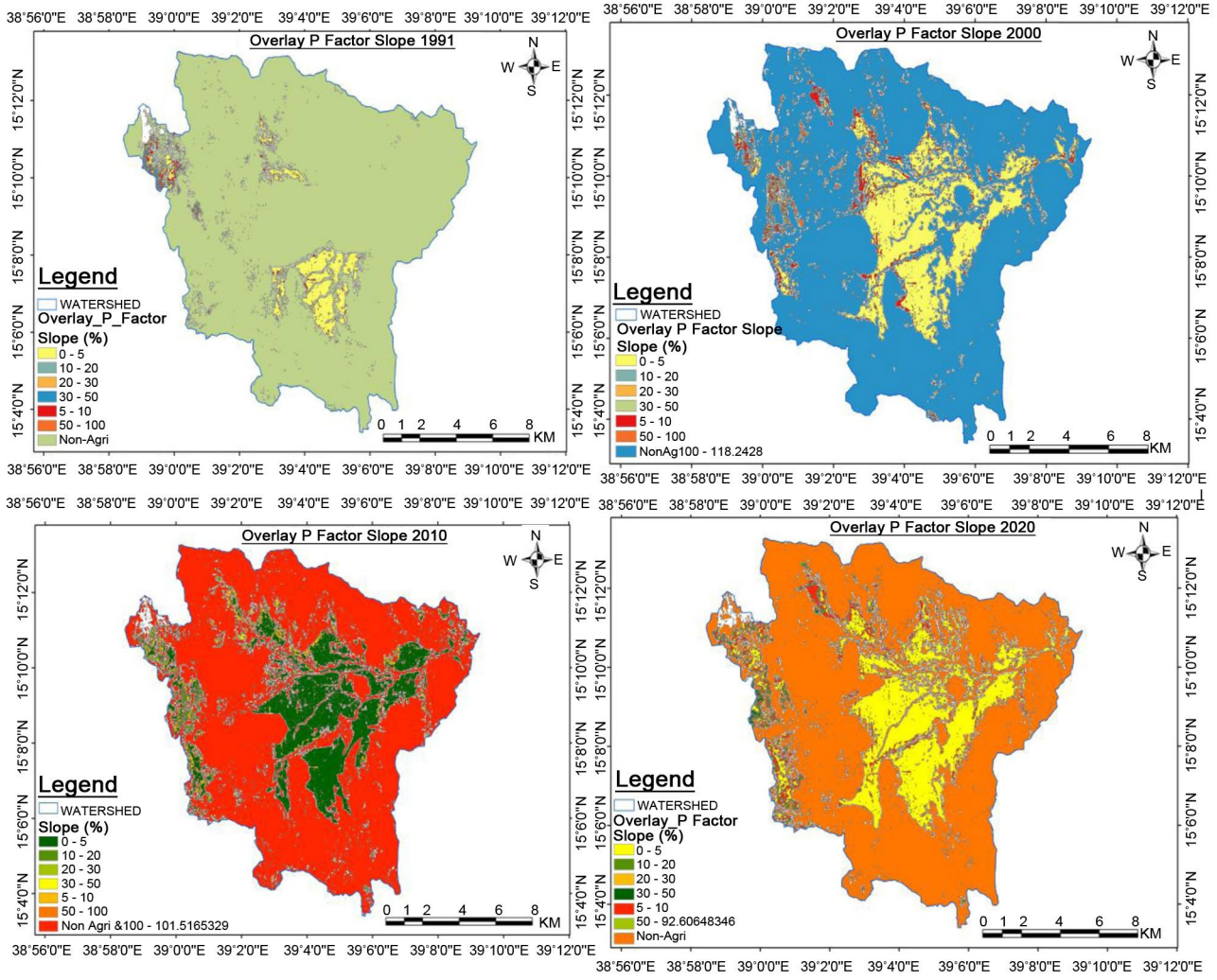

Figure 9. Slope overlay maps (1991, 2000, 2010, 2020).

non-agricultural lands. The findings continue to show an increase in agricultural land from 1991 to 2020.

Figure 10 below shows the Annual Soil Loss for the years 1991, 2000, 2010 and 2020. Based on the values obtained for R, K, LS, C, and P, the annual soil loss (A) in tons per hectare per year (t/ha/yr) was calculated for each of the four years in the study area.

The results show that in 1991, the annual soil loss ranged from 0.6062 to 51.53 t/ha/yr; in 2000 from 0.5775 to 29.45 t/ha/yr; in 2010 from 0.8335 to 53.14 t/ha/yr and in 2020 from 0.9905 to 63.14 t/ha/yr. Evidently, the highest soil loss was recorded in 2020, an indication that this year experienced the most severe land degradation due to soil erosion.

In determining the land degradation due to desertification, the NDVI, VCI, and SAVI were computed for each year considered namely 1991, 2000, 2010 and 2020 and the results are presented in Figures 11-13 respectively. According to the results, the year 2020 exhibited the lowest NDVI values, indicating sparse or

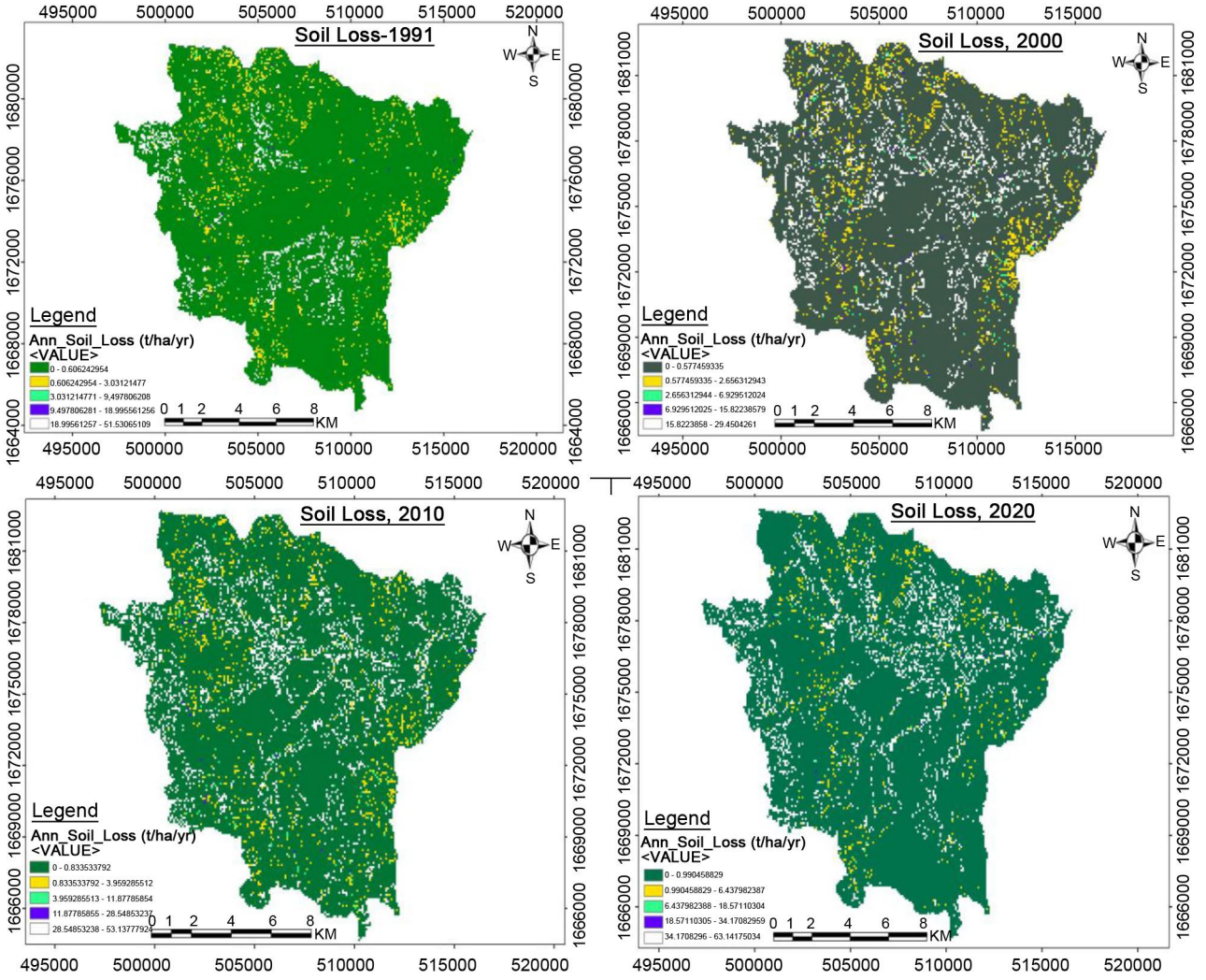

Figure 10. Annual soil loss maps (1991, 2000, 2010, 2020).

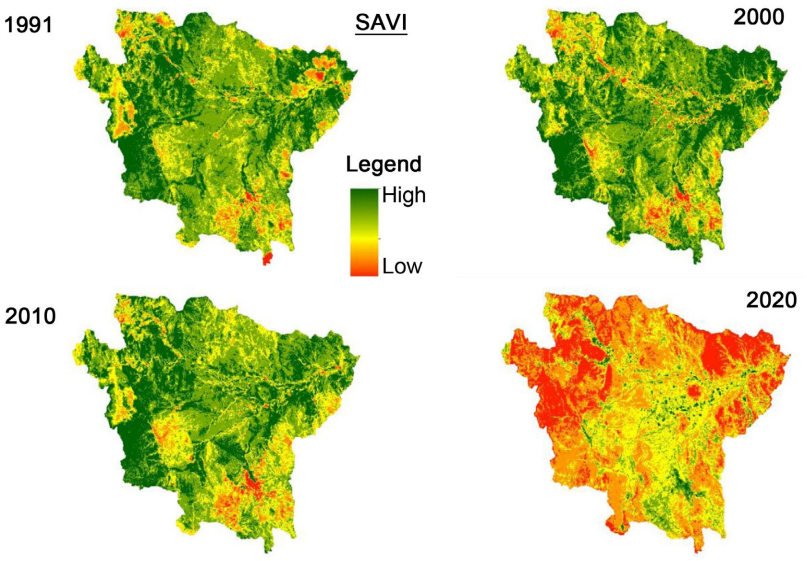

Figure 11. Desertification from NDVI (1991, 2000, 2010, 2020).

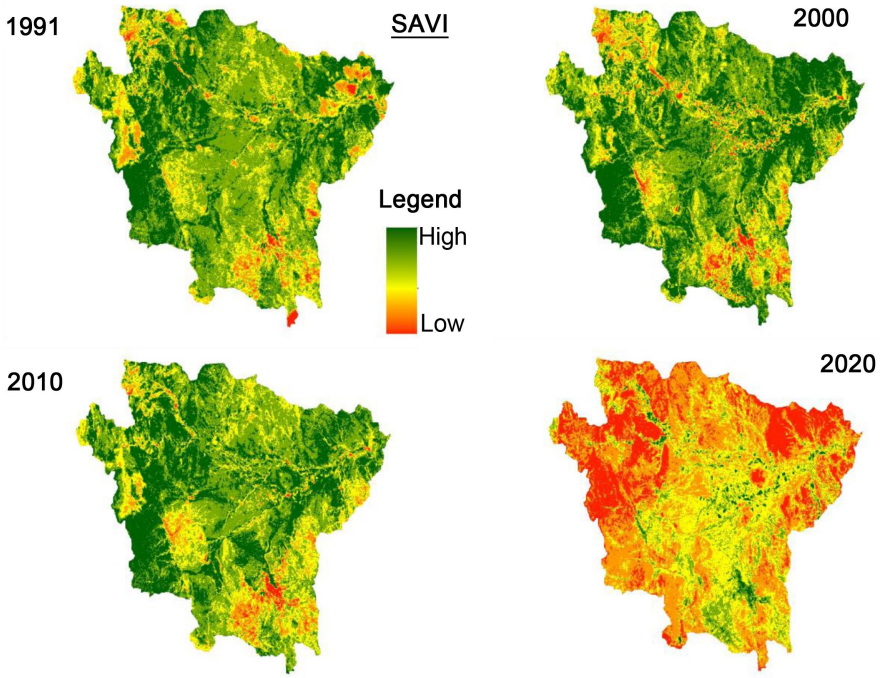

Figure 12. Desertification from SAVI (1991, 2000, 2010, 2020).

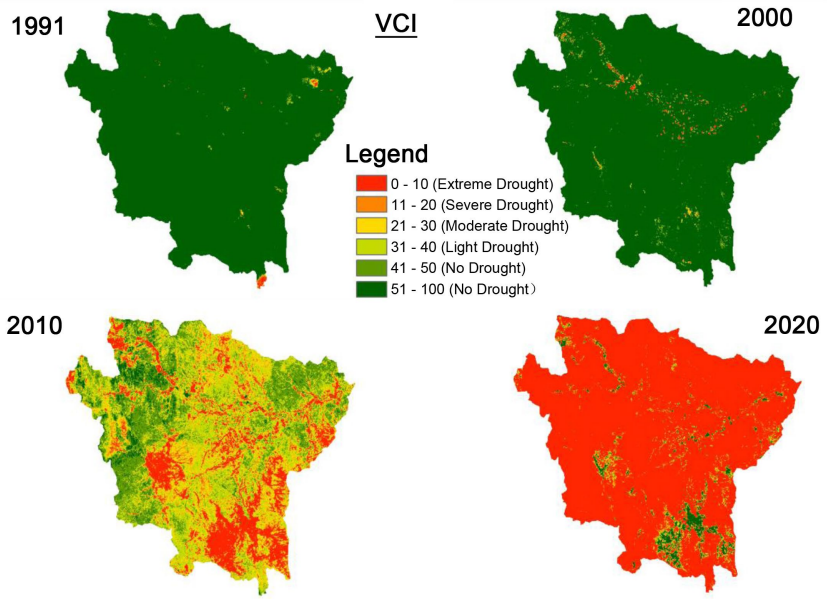

Figure 13. Desertification from VCI (1991, 2000, 2010, 2020).

stressed and unhealthy vegetation. Additionally, it showed the lowest VCI values, pointing to very poor vegetation health and severe stress, likely caused by extreme weather conditions, drought, or other adverse environmental factors. The SAVI values were also at their lowest, suggesting very sparse vegetation or bare soil, which could be attributed to arid conditions, drought, or minimal plant growth. Consequently, 2020 was identified as the worst year with respect to land degradation due to desertification.

In determining the land degradation due to desertification, the NDVI, VCI, and SAVI were computed for each of years considered in the study. According to the results, the year 2020 exhibited the lowest.

Normalized Difference Vegetation Index (NDVI) values, indicated thatsparse or stressed and unhealthy vegetation.

The Soil Adjusted Vegetation Index (SAVI) values of the year 2020 were also at their lowest levels, suggesting that very sparse vegetation or bare soil, which could be attributed to arid conditions, drought, or minimal plant growth.

Additionally, the results in 2020 showed the lowest Vegetation Condition Index (VCI) values, pointing to very poor vegetation health and severe stress, likely caused by extreme weather conditions, drought, or other adverse environmental factors.

3.2. Land Degradation Maps

By integrating the final values from the RUSLE model (annual soil loss in t/ha/yr) and desertification status (NDVI values), land degradation status maps were created for each of the four years. Since desertification, as indicated by NDVI values, has a more significant impact on land degradation than soil erosion, the desertification factor was given greater weight in the analysis. This approach ensured that the maps more accurately reflected the severity of land degradation influenced predominantly by desertification. **Figure 14** presents the land degradation maps for the years 1991, 2000, 2010 and 2020 whereas **Table 2** is a summary of the percentage of land degradation status.

Ultimately, the results revealed that the year 2020 experienced the most severe land degradation status in the study area. This conclusion was drawn from the comprehensive analysis combining RUSLE model values and NDVI-based desertification status, highlighting 2020 as the year with the most significant deterioration in land quality.

3.3. Land Degradation Susceptibility Map

From the results obtained, this study observed that most parts of the Alla catchment experience high to very high degradation status. The areas experiencing low and very low degradation status are notably vegetated. It was also noted that desertification was the major contributing factor to land degradation due to deforestation, the prolonged 30-year war for independence, and climate change that caused the drought around the area and all over the country. It was followed by soil loss due to soil erosion by surface runoff occasioned by heavy rainfall from the highland plateaus.

However, while evaluating the key parameters that resulted in the final land degradation map as outlined by RUSLE, the leading factor to soil erosion in the catchment area was found to be the Cover and management factor (C), Slope length and steepness factor (LS), Soil erodibility factor (K), Rainfall Erosivity factor (R), and Support and practice factor (P) in that order. **Figure 15** is a map

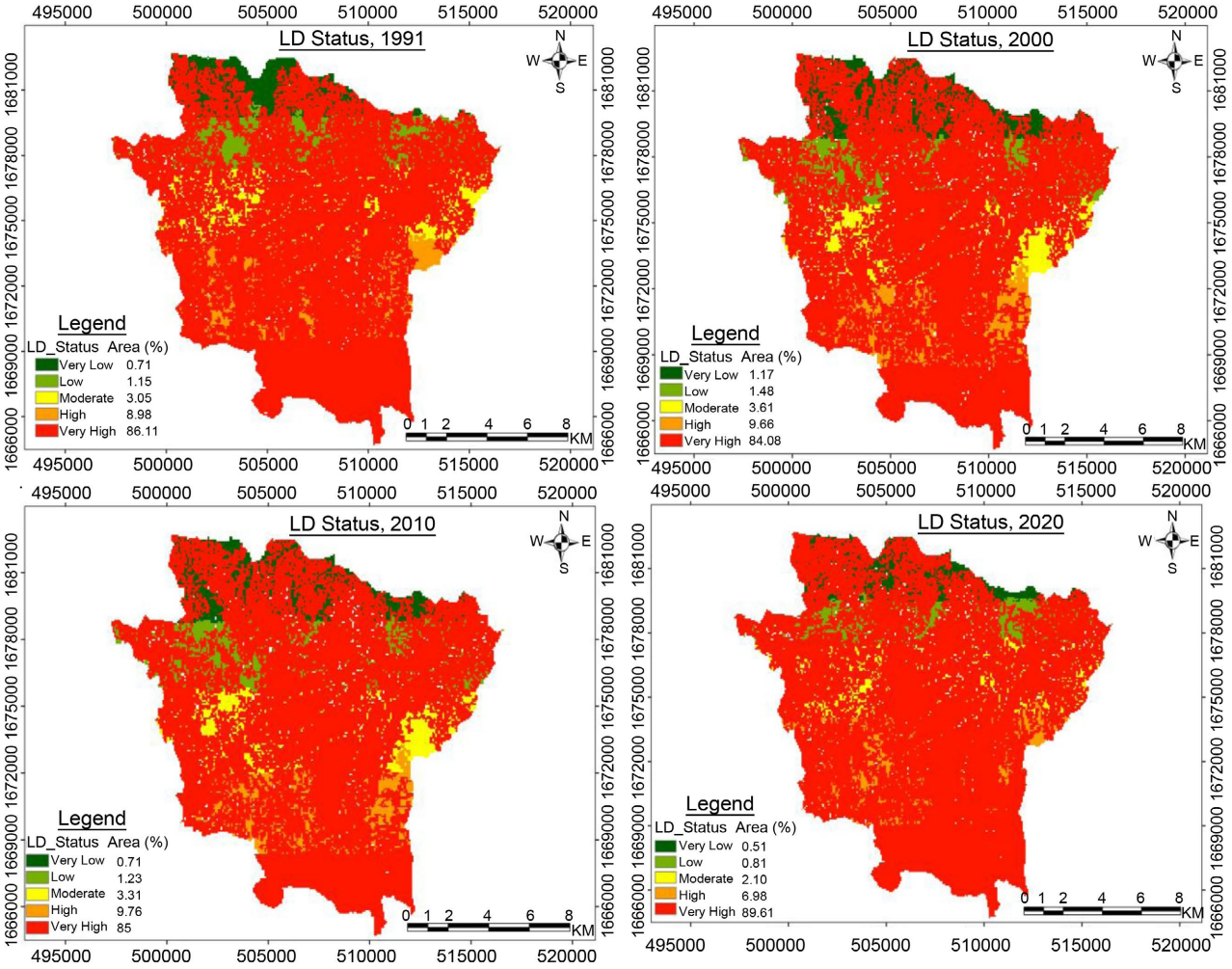

Figure 14. Land degradation maps (1991, 2000, 2010, 2020).

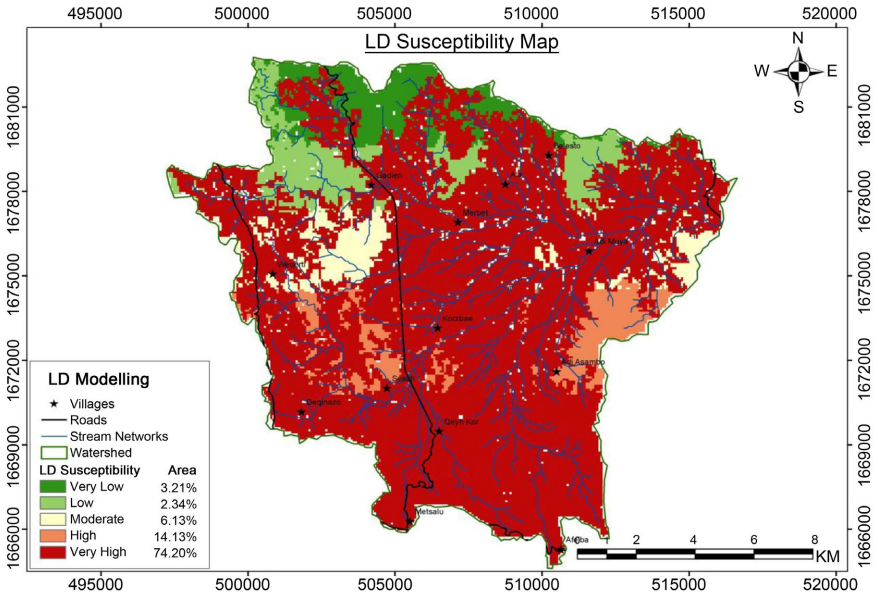

Figure 15. Land degradation susceptibility for the Alla catchement.

Table 2. Land degradation status of each year in percentage of the total study area.

	Land degradation status (% of the total catchment area)				
Year	Very low	Low	Moderate	High	Very high
1991	0.71	1.15	3.05	8.98	86.11
2000	1.17	1.48	3.61	9.66	84.08
2010	0.71	1.23	3.31	9.76	85
2020	0.51	0.81	2.10	6.98	89.61

Table 3. Land degradation susceptibility level, in percentage of the total study area.

	Land degradation susceptibility level (% of the total catchment area)				
	Very low	Low	Moderate	High	Very high
Area	3.21	2.34	6.13	14.13	74.20

showing the land degradation susceptibility status with Table 3 providing a summary in percentage area.

During 2020, the analysis of the study area's soil erosion and land degradation indicators revealed heightened risks and instances of severe degradation. Key factors such as the highest recorded Rainfall Erosivity (R-factor) values (210.012 to 251.093) and peak Soil erodibility (K-factor) values (0.3 to 0.8) indicated significant rainfall events and increased soil susceptibility to erosion. Additionally, the lowest NDVI values reflected a severe decline in vegetation health and density, reducing soil protection against erosion. This convergence of high R and K factors with poor vegetation health created an environment highly susceptible to land degradation through soil erosion and desertification. The increased agricultural land and decreased shrub lands further exacerbated these conditions. Therefore, the study has shown that the majority of the study area is under the case of high and very high land degradation susceptibility status. These findings underscore the urgent need for soil conservation measures and effective land management practices to prevent irreversible soil damage and loss of fertile land.

Applying this methodology to similar areas in Eritrea can enhance land management efforts, standardize degradation assessments, enable regional comparisons, and guide sustainable land use strategies by addressing climate, terrain, environmental and agricultural influences.

4. Conclusions

This paper demonstrates the effectiveness of an empirical land degradation model integrating the Revised Universal Soil Loss Equation (RUSLE) for soil erosion and the Normalized Difference Vegetation Index (NDVI) for desertification and drought, combined with GIS and Remote Sensing tools. Applied to the Alla catchment area, the model assessed land degradation and susceptibility over four years of 10 years intervals, highlighting spatial differences in soil loss and severity of

desertification and drought. Key drivers of soil loss were identified as the Cover and management factor (C), Slope length and steepness factor (LS), Soil erodibility factor (K), Rainfall erosivity factor (R), and Support practice factor (P). The study achieved its objectives by mapping land degradation variations from 1991 to 2020 and modelling degradation, confirming human activities and climate fluctuations as primary causes. The findings provide valuable information for decision-makers and civil society to guide restoration efforts.

The land degradation susceptibility maps and annual soil loss calculations were validated using expert inquiries and cross-referencing with data from online Google Earth.

Acknowledgements

The authors would like to acknowledge the support from the Ministry of Agriculture of the State of Eritrea, through the Vita (DeSIRA project), which played a vital role for the study as well as the Regional Centre for Mapping of Resources for Development (RCMRD) for the research funding. In addition, a deep appreciation to the Eritrean Mapping and Information Centre (EMIC) and the Southern Regional Administration Office, the State of Eritrea, for providing essential data sources that significantly contributed to the analysis.

Conflicts of Interest

The authors declare no conflicts of interest regarding the publication of this paper.

References

[1] Minelli, S., Erlewein, A. and Castillo, V. (2017) Land Degradation Neutrality and the UNCCD: From Political Vision to Measurable Targets. In: Ginzky, H., *et al.*, Eds., *International Yearbook of Soil Law and Policy*, Springer International Publishing, 85-104. https://doi.org/10.1007/978-3-319-42508-5_9

[2] Scherr, S.J. and Yadav, S.N. (1996) Land Degradation in the Developing World: Implications for Food, Agriculture, and the Environment to 2020. https://ageconsearch.umn.edu/record/42280/

[3] Vlek, P.L., Khamzina, A. and Tamene, L.D. (2017) Land Degradation and the Sustainable Development Goals: Threats and Potential Remedies. https://cgspace.cgiar.org/bitstream/handle/10568/81313/LAND_DEGRADATION_AND_THE_SDGs-THREATS_AND_POTENTIAL_REMEDIES.pdf

[4] Mitsch, W.J., Nedrich, S.M., Harter, S.K., Anderson, C., Nahlik, A.M. and Bernal, B. (2014) Sedimentation in Created Freshwater Riverine Wetlands: 15 Years of Succession and Contrast of Methods. *Ecological Engineering*, **72**, 25-34. https://doi.org/10.1016/j.ecoleng.2014.09.116

[5] Oberle, B., Bringezu, S., Hatfield-Dodds, S., Hellweg, S., Schandl, H. and Clement, J. (2019) Global Resources Outlook: 2019. International Resource Panel, United Nations Envio. https://orbi.uliege.be/handle/2268/244276

[6] Nyssen, J., Poesen, J., Moeyersons, J., Deckers, J., Haile, M. and Lang, A. (2004) Human Impact on the Environment in the Ethiopian and Eritrean Highlands—A State of the Art. *Earth-Science Reviews*, **64**, 273-320. https://doi.org/10.1016/s0012-8252(03)00078-3

[7] D'Odorico, P., Bhattachan, A., Davis, K.F., Ravi, S. and Runyan, C.W. (2013) Global Desertification: Drivers and Feedbacks. *Advances in Water Resources*, **51**, 326-344. https://doi.org/10.1016/j.advwatres.2012.01.013

[8] Bai, Z.G., Dent, D.L., Olsson, L. and Schaepman, M.E. (2008) Global Assessment of Land Degradation and Improvement: 1. Identification by Remote Sensing. ISRIC-World Soil Information. https://library.wur.nl/WebQuery/wurpubs/fulltext/40715

[9] AbdelRahman, M.A.E., Metwalli, M.R., Gao, M., Toscano, F., Fiorentino, C., Scopa, A., *et al*. (2023) Determining the Extent of Soil Degradation Processes Using Trend Analyses at a Regional Multispectral Scale. *Land*, **12**, 855. https://doi.org/10.3390/land12040855

[10] Abdelrahman, M.A.E. (2014) Assessment of Land Degradation and Land Use Planning by Using Remote Sensing and GIS Techniques in Chamarajanagar District, Karnataka. PhD Thesis, University of Agricultural Sciences.

[11] UNCCD (2017) Secretariat of the United Nations Convention to Combat Desertification. https://unfccc.int/files/parties_observers/submissions_from_observers/application/pdf/826.pdf

[12] Ghebrezgabher, M.G., Yang, T., Yang, X. and Wang, C. (2019) Assessment of Desertification in Eritrea: Land Degradation Based on Landsat Images. *Journal of Arid Land*, **11**, 319-331. https://doi.org/10.1007/s40333-019-0096-4

[13] MOA REPORT (2021) Efficient Stoves Reduce Deforestation in Eritrea. https://www.myclimate.org/en/get-active/climate-protection-projects/detail-climate-protection-projects/eritrea-efficient-cook-stoves-7121/

[14] Zeremariam, T.K. and Quinn, N. (2007) An Evaluation of Environmental Impact Assessment in Eritrea. *Impact Assessment and Project Appraisal*, **25**, 53-63. https://doi.org/10.3152/146155107x190604

[15] Swiss Data Cube (2021) The Swiss Data Cube: Earth Observations for Monitoring Switzerland's Environment in Space and Time.
SWISS DATA CUBE, 2021 Gregory Giuliani 1,2 SSDE 11 Earth and Environmental Science 509 (2020) 012021 DOI: 10.1088/1755-1315/509/1/01/2021

[16] Giuliani, G., Egger, E., Italiano, J., Poussin, C., Richard, J. and Chatenoux, B. (2020) Essential Variables for Environmental Monitoring: What Are the Possible Contributions of Earth Observation Data Cubes? *Data*, **5**, Article 100. https://doi.org/10.3390/data5040100

[17] Zerihun, M., Mohammedyasin, M.S., Sewnet, D., Adem, A.A. and Lakew, M. (2018) Assessment of Soil Erosion Using RUSLE, GIS and Remote Sensing in NW Ethiopia. *Geoderma Regional*, **12**, 83-90. https://doi.org/10.1016/j.geodrs.2018.01.002

[18] Belasri, A. and Lakhouili, A. (2016) Estimation of Soil Erosion Risk Using the Universal Soil Loss Equation (USLE) and Geo-Information Technology in Oued El Makhazine Watershed, Morocco. *Journal of Geographic Information System*, **8**, 98-107. https://doi.org/10.4236/jgis.2016.81010

[19] Prince Edward Island, Canada (2002) Revised Universal Soil Loss Equation.

[20] Stone *et al*. (2000) Rainfall Erosivity Factors.

[21] Fagnano, M., Diodato, N., Alberico, I. and Fiorentino, N. (2012) An Overview of Soil Erosion Modelling Compatible with RUSLE Approach. *Rendiconti Lincei*, **23**, 69-80. https://doi.org/10.1007/s12210-011-0159-8

[22] Verburg, P.H., Erb, K., Mertz, O. and Espindola, G. (2013) Land System Science: Between Global Challenges and Local Realities. *Current Opinion in Environmental*

Sustainability, **5**, 433-437. https://doi.org/10.1016/j.cosust.2013.08.001

[23] Ashiagbor, G. (2013) Modeling Soil Erosion Using RUSLE and GIS Tools. *International Journal of Remote Sensing & Geoscience*, **2**, 7-17. https://www.academia.edu/4125106/MODELING_SOIL_EROSION_USING_RUSLE_AND_GIS_TOOLS

[24] Atoma, H., Suryabhagavan, K.V. and Balakrishnan, M. (2020) Soil Erosion Assessment Using RUSLE Model and GIS in Huluka Watershed, Central Ethiopia. *Sustainable Water Resources Management*, **6**, Article No. 2. https://doi.org/10.1007/s40899-020-00365-z

[25] Anache, J.A.A., Bacchi, C.G.V. and Sobrinho, T.A. (2015) Assessment of Methods for Predicting Soil Erodibility in Soil Loss Modeling. *Geociências*, **34**, 32-40.

[26] Endalamaw, N.T., Moges, M.A., Kebede, Y.S., Alehegn, B.M. and Sinshaw, B.G. (2021) Potential Soil Loss Estimation for Conservation Planning, Upper Blue Nile Basin, Ethiopia. *Environmental Challenges*, **5**, 100224. https://doi.org/10.1016/j.envc.2021.100224

[27] Tsegaye, L. and Bharti, R. (2021) Soil Erosion and Sediment Yield Assessment Using RUSLE and GIS-Based Approach in Anjeb Watershed, Northwest Ethiopia. *SN Applied Sciences*, **3**, Article No. 582. https://doi.org/10.1007/s42452-021-04564-x

[28] Karaburun, A. (2010) Estimation of C Factor for Soil Erosion Modeling Using NDVI in Buyukcekmece Watershed. https://www.semanticscholar.org/paper/Estimation-of-C-factor-for-soil-erosion-modeling-in-Karaburun/7165721e2f730d5191d9f0d8fea7eca586e5e224

[29] Gelagay, H.S. and Minale, A.S. (2016) Soil Loss Estimation Using GIS and Remote Sensing Techniques: A Case of Koga Watershed, Northwestern Ethiopia. *International Soil and Water Conservation Research*, **4**, 126-136. https://doi.org/10.1016/j.iswcr.2016.01.002

[30] Wischmeier and Smith. P Values. https://www.researchgate.net/figure/P-values-Wischmeier-and-Smith-1978_tbl3_318256013